ChemCatChem

The European Society Journal for Catalysis

Chemistry Europe

European Chemical Societies Publishing

Supported by GECATS GERMAN CATALYSIS SOCIETY

# Accepted Article

**Title:** Insights into the Suzuki-Miyaura Reaction Catalyzed by Novel Pd – Carbene Complexes. Are Palladium – Tetracarbene Entities the Key Active Species?

**Authors:** Jonathan De Tovar, Franck Rataboul, and Laurent Djakovitch



**To be cited as:** *ChemCatChem* 10.1002/cctc.202001253

**Link to VoR:** https://doi.org/10.1002/cctc.202001253

WILEY-VCH

10.1002/cctc.202001253

WILEY-VCH

FULL PAPER

# Insights into the Suzuki-Miyaura Reaction Catalyzed by Novel Pd – Carbene Complexes. Are Palladium – Tetracarbene Entities the Key Active Species?

Jonathan De Tovar,*[a] Franck Rataboul[a] and Laurent Djakovitch*[a]

[a] Dr. Jonathan De Tovar, Dr. Franck Rataboul, Dr. Laurent Djakovitch
Université de Lyon, Université Claude Bernard Lyon 1, CNRS, IRCELYON
F-69626, Villeurbanne, France
E-mail: Jonathan.DeTovar@ircelyon.univ-lyon1.fr; Laurent.Djakovitch@ircelyon.univ-lyon1.fr

Supporting information for this article is given via a link at the end of the document.

**Abstract:** The assumption that the real active species involved in the Suzuki-Miyaura reaction are homogeneous, heterogeneous or both is often proposed. However a lack in the characterization of true catalytic entities and their monitoring makes assumptions somewhat elusive. Here, three families of palladium(II) complexes bearing bisNHC, bispyridyl and bisphosphine ligands were synthesized in order to get new insights into the formation of active species in the Suzuki-Miyaura reaction. Their comparative catalytic study reveals that the nature of the ligands as well as their spacer lengths are pivotal parameters governing the performance. All complexes evolve to Pd NPs under reaction conditions, and an orthogonal behavior is observed for two bisNHC complexes that form homoleptic tetracarbene species. Notably, these species are presumably involved in a new catalytic modus operandi. This ligand-controlled reactivity and the formation of tetracarbene species open new routes towards the design of novel cross-coupling catalysts via the mastering of highly-active catalytic species.

## Introduction

Palladium-catalyzed cross-coupling reactions are of paramount importance from an industrial point of view.[1] In particular, the Suzuki-Miyaura reaction allows to easily form biaryls intermediates useful in organic synthesis.[2] This reaction is catalyzed mainly using palladium species giving generally high activities.

Well-defined palladium molecular complexes and nanoparticles (NPs) have been used for this reaction.[3] A controversy concerning the exact nature of the real catalytic system (the catalytic active species) exists under turnover conditions.[4-6] For instance, very active catalytic species such as NPs or metal clusters evolved from molecular complexes are quite often postulated by the metal – ligand cleavage. [7,8]

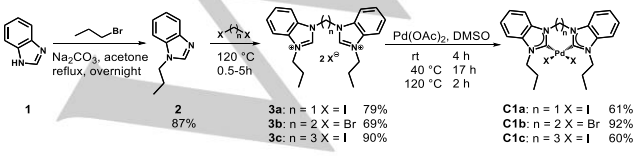


**Scheme 1.** Synthetic pathway for **3a-c** ligands and **C1a-c** complexes.

In molecular complexes, the structure and electronic properties of the ligand coordinated to the metal core are pivotal factors influencing not only the activity, selectivity and stability of the catalysts[9,10] but also their evolution to the real catalysts or depletion to bulk palladium.[11] Due to the good stability and coordination capability, pyridyls serve as *N*-ligands for some transition metal-catalyzed reactions, especially redox reactions.[12,13] In addition, as an alternative to phosphines, the remarkably strong σ–binding and π-backdonation characters, steric tunability and high stability under oxidative conditions of *N*-heterocyclic carbene (NHC) ligands, provide them the ability to stabilize highly unusual and hitherto elusive reactive species such as metal nanoparticles.[14,15] Nevertheless, despite the Pd-NHC complexes have been considered as robust catalysts, the M-NHC bond is susceptible to facile cleavage by reactions of reductive elimination, protonolysis and ligand displacement, which prompts to unravel the *modus operandi* of such systems.[8d] Chelating ligands are believed to provide additional catalyst stability under turnover conditions, and several studies describe the preparation and applications of biscarbene-bridged palladium(II) complexes in such C-C coupling reactions.[16-23] For example, Jothibasu and Huynh prepared a series of palladium(II) complexes bearing *cis*-chelating *homo-dicarbene* ligands varying bridges and N-heterocyclic backbones. Results for the Mizoroki-Heck reaction revealed superior activities for methylene- and propylene- bridged dibenzimidazol-2-ylidenes ligands.[21] However, although some general trends have been introduced for the Mizoroki-Heck reaction, a deep study based on the spacer-length unit, ligand nature, substrate and temperature has not been, to the best of our knowledge, reported for the Suzuki-Miyaura reaction.

In this work we studied the evolution of palladium complexes of the type $PdX_2(L\cap L)$, in which L∩L is a chelating bis(benzimidazol-2-ylidene) ligand, in the Suzuki-Miyaura reaction to identify the nature of the active species generated from such complexes. For that we particularly evaluated (a) the effect of the spacer-length (∩), (b) the influence of the coordination ligand, (c) the nature of the substrate and (d) the effect of the temperature. For this comparison we also studied the influence of bispyridyl and bisphosphine ligands. Indeed, one can speculate that Pd species in the reaction medium can be controlled by the nature of the selected bidentate ligands from which it is expected an easier decoordination for bisphosphine ligands relative to bispyridyl and biscarbene ligands under same reaction conditions.

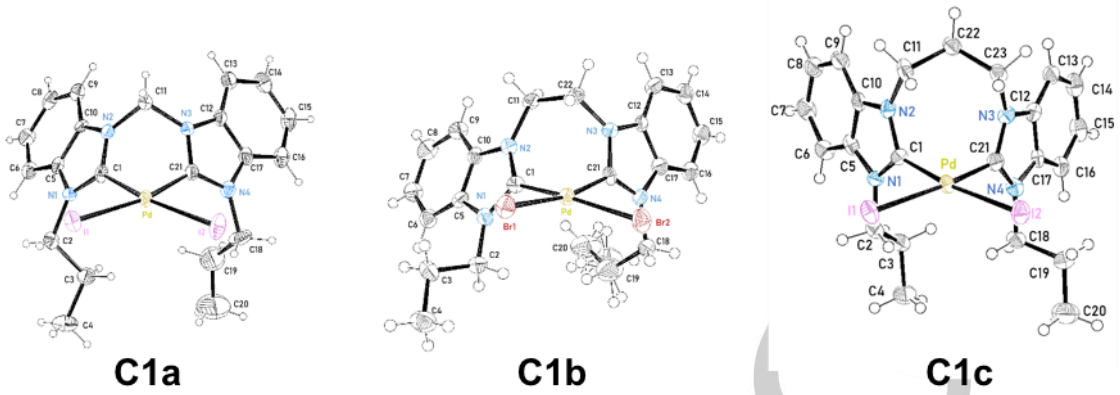


**Figure 1.** Displacement ellipsoid plots of **C1a-c** complexes at the 50% probability level. Solvent molecules are omitted for clarity.

## Results and Discussion

**Synthesis and Characterization of Bidentate-Ligands and Complexes.** The synthetic strategy followed for the preparation of ligands is outlined in Scheme 1. It is based on alkylation of benzimidazole with bromopropane followed by a subsequent substitution reaction with different dihaloalkanes. Ligands **3a-c** were fully characterized by NMR (1D and 2D spectra, see Experimental section and Figures S1-S3). $^1$H NMR spectra indicate a C2 symmetry in solution for the three ligands in which not only the two alkylated benzimidazolium moieties are equivalent but also the bridge protons. All ligands have also been characterized by HR-ESI-MS (Figures S4-S6) and IR spectroscopy (Figures S7-S9).

Palladium(II) molecular complexes of **3a-c** have been synthesized in order to evaluate the coordination properties of these ligands as well as their influence when resulting Pd complexes were engaged in the Suzuki-Miyaura reactions. **C1a-c** were prepared following the temperature program of Ahrens *et al.*[24] directly reacting palladium(II) acetate with the different bisbenzimidazolium salts in hot DMSO (Scheme 1).

All Pd(II) complexes have been obtained as air- and moisture-stable solids. $^1$H NMR spectra of **C1a-c** complexes show that the downfield signals (9-11 ppm) of acidic protons for the different bisbenzimidazolium salts are no longer present (Figures S10-S12), thus confirming the deprotonation of the benzimidazolium moiety and formation of biscarbene complexes. Additionally, all methylene protons of the bridges become diastereotopic due to ligand coordination and retention of the bend-boat conformation in these complexes.[17] The observed broadening of these resonances has been attributed to the fluxionality of the seven- or eight-membered chelate rings.[21] Interestingly, the methylene protons of propyl chains became also diastereotopic because of the H···X interaction with iodo or bromido ligands, these methylene protons being shifted downfield (4-5 ppm). Scherg *et al.* prepared similar complexes and determined high coalescence temperatures at which the inequivalent protons become isotopic.[17] The formation of the **C1a-c** mononuclear complexes is supported by their ESI high-resolution mass spectra at *m/z* = 565.0075 and 593.0384 for the molecular cations $[M-I]^+$ (**C1a** and **C1c**, respectively, Figures S13 and S15), and 533.0358 for the molecular cation $[M-Br]^+$ (**C1b**, Figure S14), which fit with their simulated spectra. Finally, the formation of the complexes has been attested by IR spectroscopy (Figures S16-S18).

Single crystals suitable for X-ray diffraction analyses for **C1a-c** complexes were obtained by slow evaporation (1 month) in the fume hood at room temperature of saturated DMF solutions (1 mL) for **C1a** and **C1c** and a saturated DMSO solution (1 mL) for **C1b**. Molecular plots of **C1a-c** are shown in Figure 1, and selected crystallographic data, bond distances and angles are collected in Tables S1 and S2. The whole **C1a-c** complex family crystallized in a monoclinic crystal system. All complexes show a *cis*-geometry around a slightly distorted square-planar palladium center, with the two halides twisted out of the $PdC_2$ plane by 3.5(9)-11.2(1)°. The Pd-C coordination bond lengths in the three complexes are rather similar and in agreement with those in similar complexes reported before.[21] The C1-Pd-C21 bite angle changes slightly upon lengthening of the bridging moiety, from 82.4(3)° for **C1a** to 86.1(3)° and 85.1(3)° for **C1b** and **C1c**, respectively. Compared to the chelating bisdiphenylphosphino alkanes, where every additional methylene moiety in the bridging chain leads to an increase in bite angle of 4.8-13.1°, this is a relatively small difference.[26] This smaller effect in the bite angle is due to the angle at which the benzimidazole rings are twisted relative to the coordination plane (Table S1),[26] being quasi perpendicular for longer bridging moieties.[24] This indicates a greater steric demand by the ligands that is supported by the distance of the propyl groups, which shields the metal from the lower side of the complex.[26] Accordingly, the distance became shorter with growing bridge length (**C1a**: 3.584, 3.606 Å, **C1b**: 3.381, 3.546 Å; **C1c**: 3.477, 3.493 Å). The most important feature of these structures are the interactions between protons from bridge or propyl chain and palladium(II) core (C-H···Pd, Figures S19-S21). For **C1b**, the bond lengths and angles indicate pure agostic interactions since the distance between the hydrogen atoms and the palladium(II) core is shorter than the sum of their van der Waals radii. However, for **C1c** complex, the bond lengths and angles indicate that these interactions are anagostic.[29] Interestingly for **C1a**, although the distance of Pd and the H11a bridge proton is larger than the sum of their van der Waals radii, the angle of 87.03° and the fixed boat conformation indicate a pseudo-agostic interaction. Nevertheless, the presence of all these weak interactions supports the downfield shift of the methylene moieties in the $^1$H NMR spectra (*vide supra*). The

10.1002/cctc.202001253




bridges and propyl chains show staggered conformations along their bonds, as expected. Details of the structure determinations are given in the Experimental section and Supplementary material (Appendix A). Note that the **C1a-c** complexes could not be prepared by using the dichloroalkanes although their preparation was attempted.

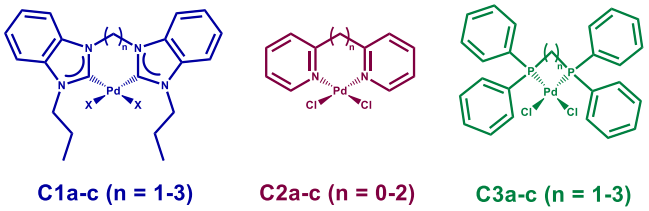


**Figure 2.** Pd(II) complexes used as catalysts in this work.

As indicated above, with the aim of evaluating the nature of the ligand, bispyridyl-based **C2a-c** and bisphosphine-based **C3a-c** complexes (Figure 2) have been prepared for comparison purposes following reported procedures.[25,29,30]

**Catalytic Performance in the Suzuki-Miyaura Reaction**. The different prepared palladium(II) complexes have been evaluated as catalysts for the model reaction depicted in Scheme 2. We aimed at performing the reactions under mild conditions and short times using low catalyst loading.

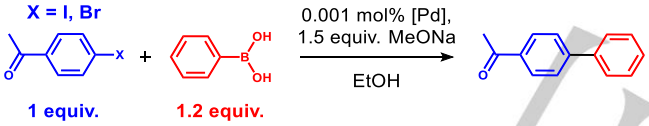


**Scheme 2.** Suzuki-Miyaura reaction studied in this work.

*p*-Halogenoacetophenone derivatives and phenylboronic acid were selected as substrates in order to easily distinguish between cross-coupling and homocoupling products. In all experiments, neither homocoupling of phenylboronic acids nor homocoupling of aryl halide or dehalogenation of *p*-halogenoacetophenone were observed. Thus, since the formation of *p*-acetylbiphenyl was exclusive, we considered yields equal to conversion values.

In order to compare the effect of the nature of the ligands for the different catalysts, experiments were performed at different reaction temperatures measuring the catalytic performance. The results obtained were compared to those achieved using the Herrmann-Beller (HB) palladacycle pre-catalyst.[32]

The evolution of the conversion of *p*-halogenoacetophenones with time was determined at 60 °C and 25 °C (Figures 3-4). Final conversions, Turnover numbers (TONs), Turnover-frequencies (TOFs), initial activities (iTOFs) and evolution of activities with their induction periods were determined for each reaction conditions and reported in Tables 1 and 2 (see Experimental Section for further details).

As a general trend, higher conversions were obtained with *p*-iodoacetophenone (Table 2), as expected from the respective C-X bond energies.[32]

First, for *p*-iodoacetophenone at 60 °C (Figure 3, Table 1), complete conversions were achieved after 1 h in all cases. Figure 3 shows that, independently of ligand nature, the length of the bridging unit had an influence. For the three families of catalysts the longer the bridging chain is, the higher iTOFs is obtained. This effect is more pronounced for bisphosphine-based ligands where **C3a**, **C3b** and **C3c** exhibited iTOFs of 280, 1208 and 1830, respectively (Figure 3c, Table 1 entries 7-9). As expected, decreasing the temperature to 25 °C (Figure 4, Table 1) resulted in lower initial activities for all catalysts. Importantly, the catalysts seem to evolve to different Pd-species since their catalytic activities (A2) dramatically changed after some minutes (induction periods) at 25 °C (Figure 4, Table 1). Remarkably, the kinetic curves for **C1a** and **C1b** catalysts demonstrate a sigmoid plot that indicates possible catalyst activation (Figure 4a). Thus, their catalytic activity increase with time while it decreases for **C1c**. As a result, since **C2a-c** and **C3a-c** follow the same trend observed at 60 ºC, higher conversions are achieved with smaller chelates for **C1a-c** (Figure 4a, Table 2 entries 1-3). Although this phenomenon is not observed at 60ºC maybe due to reaction running too fast, it can be inferred that the different catalytic performance of **C1a-c** complexes at 25ºC reveals a crucial role of NHC ligands.

This behavior is very similar to that observed for Herrmann-Beller complex (Figure S42, Table 1 and Table 2) that is reputed to deliver Pd NPs in the reaction mixture after relative short period of time as shown by Louie *et al.*[33] Interestingly, the new **C1a-c** catalysts prepared here exhibited higher initial activities than that of the Herrmann-Beller palladacycle catalyst (Table 1 and Table 2 entries 1, 2 and 3 versus entry 10).

**Evolution of Pd species during the catalytic reactions.** Recently, Astakhov *et al.*[34] demonstrated the formation of Pd NPs when molecular Pd complexes with NHC ligands are used in the Mizoroki-Heck reaction. In our case, TEM analyses of the reaction after catalytic runs show the presence of Pd NPs for all **C1a-c** catalysts (Figure 5 and Table S3). Two families of Pd NPs of *ca.* 3.7 ± 1.1 and 11.6 ± 1.8 nm could be found for **C1a**, a single family of *ca.* 10.6 ± 1.6 nm for **C1b** and two families of *ca.* 9.8 ± 2.3 and 63.1 ± 11.9 nm for **C1c**. Thus, size-dependent catalytic activity of the evolved Pd NPs from **C1a-c** can be rationalized: increased catalytic activities is observed with decreasing NPs size. Additionally, the **C2a-c** complexes evolved to Pd NPs under turnover conditions exhibiting higher iTOFs for smaller nanoparticles (Figure S44, Tables 1 and S3).

Contrary to **C1a-c** and **C2a-c**, Pd NPs evolved from **C3a-c** complexes (Figure S44 and Table S1) exhibited higher activities for larger NPs sizes. This can be explained by the different coordination modes of the ligands at the Pd NPs surface. On the one hand, carbene and pyridyl-based ligands of **C1a-c** and **C2a-c** can stabilize nanoparticles both by σ- and π- interactions.[8d,35] More to this point, metal-to-carbene π-backdonation can be responsible for up to 20- 30% of total M-to-C bond strength in transition metal-NHC entities.[36-38] On the other hand, although **C3a-c** exhibit both σ-donation and π-backdonation like carbene-based ligands, phosphines are more labile. Then, since all bisphosphine ligands in **C3a-c** exhibit similar Tolman's cone angles,[39] when increasing the bridge length, the bite angle becomes wider while stabilizing nanoparticles because of their

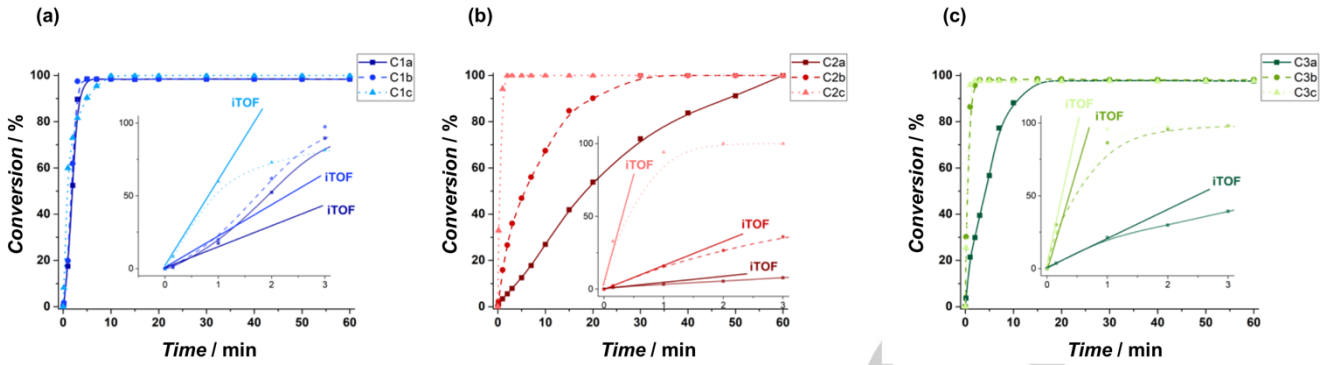


**Figure 3.** Conversion versus the time for the coupling reaction of *p*-iodoacetophenone with phenyl boronic acid using (a) **C1a-c**, (b) **C2a-c** and (c) **C3a-c** catalysts at 60 °C.

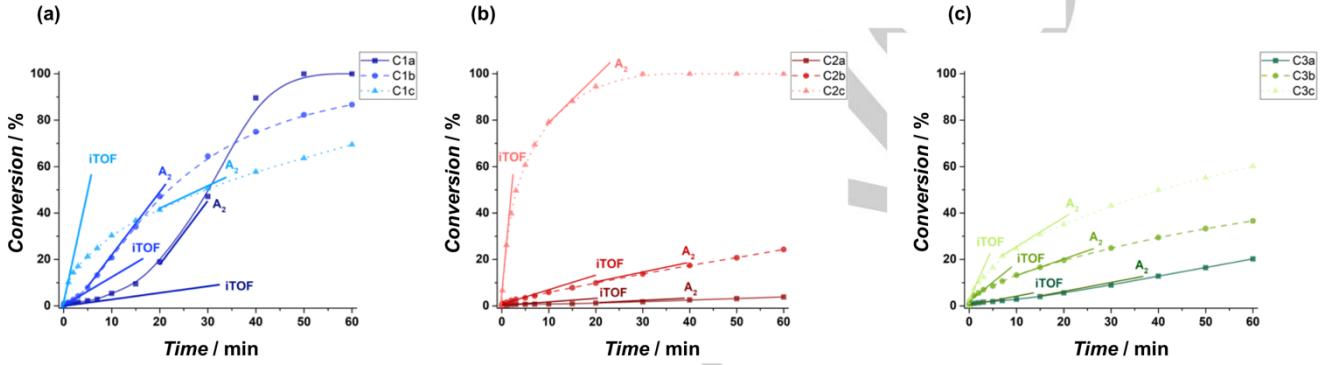


**Figure 4.** Conversion versus the time for the coupling reaction of *p*-iodoacetophenone with phenyl boronic acid using (a) **C1a-c**, (b) **C2a-c** and (c) **C3a-c** catalysts at 25 °C.

**Table 1. Catalyst activities for the Suzuki-Miyaura reaction of *p*-haloacetophenone with phenylboronic Acid.**

| Entry | Catalyst | *p*-iodoacetophenone | | | | *p*-bromoacetophenone | | |
|---|---|---|---|---|---|---|---|---|
| | | 60 °C | 25 °C | | | 60 °C | | |
| | | iTOF (mol product · mol $Pd^{-1}$ · $min^{-1}$) | iTOF (mol product · mol $Pd^{-1}$ · $min^{-1}$) | $A_2$ (mol product · mol $Pd^{-1}$ · $min^{-1}$) | Induction time (min) | iTOF (mol product · mol $Pd^{-1}$ · $min^{-1}$) | $A_2$ (mol product · mol $Pd^{-1}$ · $min^{-1}$) | Induction time (min) |
| 1 | **C1a** | 159 | 7 | 173 | 20 | 611 | stopped | 5 |
| 2 | **C1b** | 218 | 15 | 34 | 5 | 294 | stopped | 10 |
| 3 | **C1c** | 846 | 133 | 15 | 10 | 90 | stopped | 20 |
| 4 | **C2a** | 31 | 1 | 0.6 | 15 | 1 | 0.2 | 20 |
| 5 | **C2b** | 169 | 6 | 6 | 7 | 36 | 6 | 20 |
| 6 | **C2c** | 1337 | 318 | 66 | 7 | 206 | stopped | 5 |
| 7 | **C3a** | 280 | 5 | 3 | 15 | 108 | 16 | 20 |
| 8 | **C3b** | 1208 | 172 | 8 | 10 | 223 | 7 | 10 |
| 9 | **C3c** | 1830 | 229 | 6 | 7 | 240 | 22 | 10 |
| 10 | **H-B** | 106 | 3 | 26 | 20 | 254 | stopped | 20 |

Reaction conditions: 8 x $10^{-4}$ mmol Pd, 0.8 mmol *p*-haloacetophenone, 1 mmol phenylboronic acid, 1.2 mmol MeONa and 9 x $10^{-2}$ mmol naphthalene as an internal standard in 16 mL absolute EtOH.

extended conformation and further coordination to long-in-distance separate Pd atoms.[40] This may tune both electronic and steric properties at the NPs surface and consequently the catalytic behavior. TEM analyses of reaction mixture obtained at 60 °C for the same substrate revealed smaller NPs for **C1a-c** and **C2a-c** but larger for **C3a-c** complexes (Figure S43, Tables 1 and S3).

Thus, increasing the temperature could greatly enhance the complex decomposition followed by cluster formation as well as favoring the leaching of highly-active Pd species from Pd NPs. NPs formation was also observed for all catalysts when *p*-bromoacetophenone was used as substrate (Figure S45, Table S3). However, their size histograms differed from those for *p*-iodoacetophenone at 60ºC indicating that the substrate could take a pivotal role in the clusterification step and Pd leaching.

Here, three families of catalysts showed different trends. Firstly, **C1a-c** catalysts reached a plateau in the conversion in the first 5-20 minutes with highest iTOFs for smaller chelates (Figure 6a, Table 1 entries 1-3). In contrast with *p*-iodoacetophenone, TEM analyses reveal the formation of homogenous spherical Pd NPs (Figure 5 and Table S3) for the three catalysts and, as evidenced

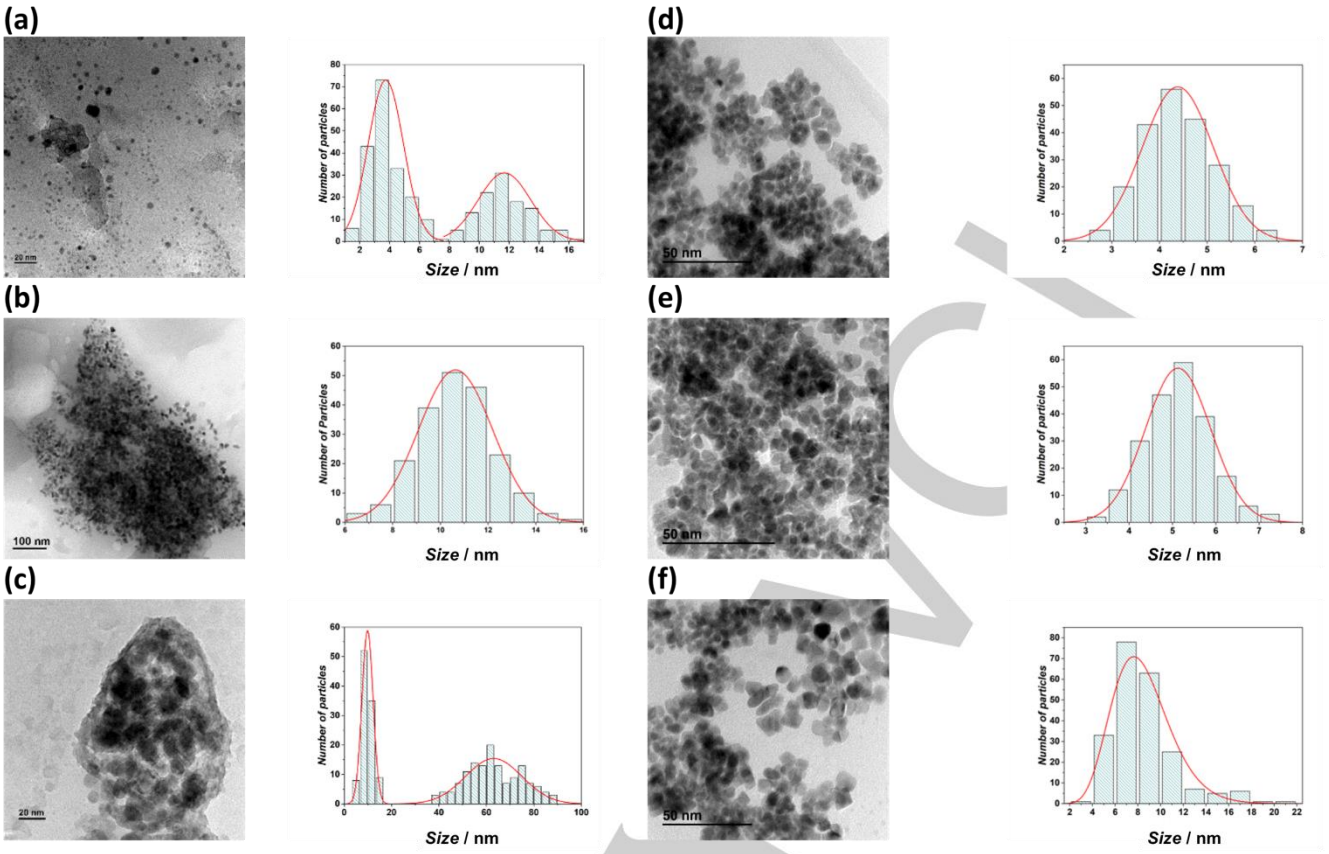


**Figure 5.** TEM micrographs and the corresponding size-histograms of Pd NPs observed after the catalytic tests with *p*-iodoacetophenone as substrate at 25 °C using (a) **C1a**, (b) **C1b** and (c) **C1c**. TEM micrographs and the corresponding size-histograms of Pd NPs observed after the catalytic tests with *p*-bromoacetophenone as substrate at 60 °C using (d) **C1a**, (e) **C1b** and (f) **C1c**.

from their size distribution histograms, larger particles are formed for longer bridges. Although this could explain their initial iTOFs, their depletion remains raveled. As the solid surface is modified with the time (*i.e.* clusterification step), the loss of activity could be due to the surface rearrangement or the degradation of Pd NPs stabilizers entities (decomposition of ligands or *in situ* generated species). Secondly, as observed for *p*-iodoacetophenone, **C2a-c** and **C3a-c** catalysts exhibited higher iTOFs for longer bridges but **C2c** activity stopped after 5 minutes.

Finally, data clearly indicates that **C1a** is more active than any other catalyst because of its faster kinetics (Table 1 entry 1). Given these catalytic evidences, it can be inferred that the catalysts performance is depending on the ligand scaffold and its nature, as well as the targeted aryl halide to be coupled. However, the nature of the active species remains raveled. All data obtained with the three complex series are compiled in Table 2.

**Elucidating the nature of active species.** Mercury poisoning tests[40] were applied to the reactions of *p*-iodoacetophenone and *p*-bromoacetophenone with phenylboronic acid under catalysis conditions with all complexes. Due to the high iTOFs exhibited by the catalysts, a large excess of Hg(0) (Hg:Pd ≈ 2000:1 mol/mol) was added to the reaction mixtures at the beginning to elucidate a molecular nature of the catalytic species. As shown in Table 2 and Table 3, the catalytic reactions ceased completely for all catalysts but some conversions were observed with **C1b**, **C1c** and **C2c** when using *p*-iodoacetophenone as substrate. Similar results were observed when using *p*-bromoacetophenone. In this case, conversions completely ceased for all catalysts despite some conversions with **C1a** and **C1b** (Table 3).

These data suggest that molecular complexes act in fact as pre-catalysts and their evolved Pd NPs act as the active species or as reservoir of molecular palladium species. Then, the conversions observed for the catalyst could be due to (a) the high activity of their evolved Pd NPs before Hg-Pd amalgam formation or (b) the generation of highly- active catalytic species. All these analyses are in accordance with the different results observed in catalysis depending on the molecular or colloidal nature of the introduced catalysts.

However, the mercury poisoning tests is not a definitive proof since the amalgam of Hg and Pd from the NPs could prevent potential Pd molecular species from leaching.[42]

TEM analyses, mercury poisoning tests and catalytic studies suggest that the key role of Pd clusters could be highlighted as "cocktail"-type behavior.[34]

These results prompted us to investigate the process of the evolution of **C1a-c** pre-catalysts whose exhibited moderate conversions in the presence of Hg and catalyst depletion when reacting with p-bromoacetophenone (Table 3).

Although NHC-based ligands are well known because of their stabilizing features under oxidative conditions, it was evidenced that Pd-NHC complexes can evolve through the cleavage of the Pd-$C_{carbene}$ bond by a C-C reductive elimination from the intermediate after the oxidative addition of aryl halides.[34] Thus, we attempted to determine the products formed during the

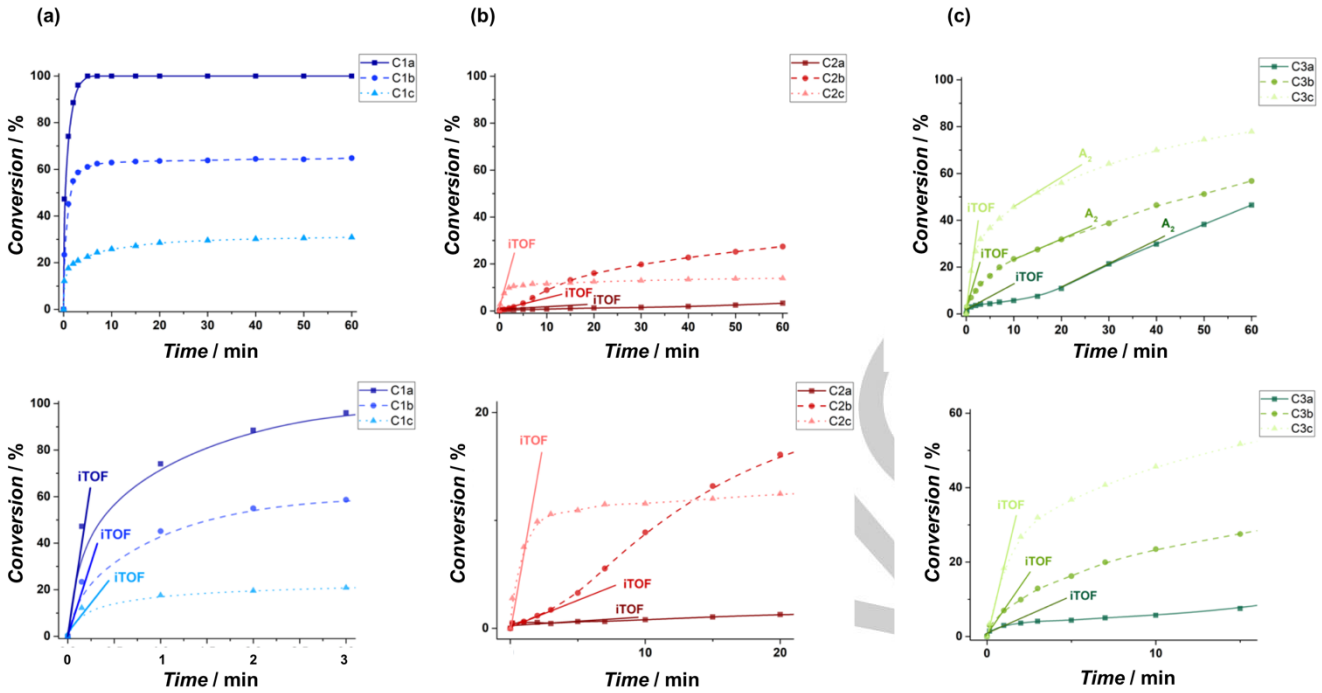


**Figure 6.** Conversion versus the time (top) and insets (bottom) for the coupling reaction of *p*-bromoacetophenone with phenyl boronic acid using (a) **C1a-c**, (b) **C2a-c** and (c) **C3a-c** catalysts at 60 °C.

**Table 2. Conversion, TON and TOF values for the Suzuki-Miyaura reaction of *p*-haloacetophenone with phenylboronic Acid.**

| Entry | Catalyst | *p*-iodoacetophenone | | | | | | *p*-bromoacetophenone | | |
|---|---|---|---|---|---|---|---|---|---|---|
| | | 60 °C | | | 25 °C | | | 60 °C | | |
| | | Conv. | TON | TOF ($h^{-1}$) | Conv.[b] | TON | TOF ($h^{-1}$) | Conv.[b] | TON | TOF ($h^{-1}$) |
| 1 | **C1a** | 100 | 1000 | 12000 | 100 | 1000 | 1200 | 100 | 1000 | 12000 |
| 2 | **C1b** | 100 | 1000 | 20000 | 87 | 867 | 867 | 65 | 648 | 3888 |
| 3 | **C1c** | 100 | 1000 | 6000 | 70 | 695 | 695 | 31 | 309 | 927 |
| 4 | **C2a** | 100 | 1000 | 1000 | 4 | 39 | 39 | 3 | 331 | 331 |
| 5 | **C2b** | 100 | 1000 | 2000 | 24 | 243 | 243 | 28 | 275 | 275 |
| 6 | **C2c** | 100 | 1000 | 30000 | 100 | 100 | 2000 | 14 | 139 | 417 |
| 7 | **C3a** | 100 | 1000 | 4000 | 20 | 203 | 203 | 47 | 465 | 465 |
| 8 | **C3b** | 100 | 1000 | 20000 | 37 | 366 | 366 | 57 | 568 | 568 |
| 9 | **C3c** | 100 | 1000 | 60000 | 60 | 602 | 602 | 78 | 779 | 779 |
| 10 | **H-B** | 100 | 1000 | 8571 | 75 | 750 | 750 | 99 | 991 | 2973 |

Reaction conditions: 8 x $10^{-4}$ mmol Pd, 0.8 mmol *p*-haloacetophenone, 1 mmol phenylboronic acid, 1.2 mmol MeONa and 9 x $10^{-2}$ mmol naphthalene as an internal standard in 16 mL absolute EtOH. Conversion after 1 h reaction.

transformation of the **C1a-c** complexes over the course of the Suzuki-Miyaura reaction. A dedicated study of the reaction between *p*-iodoacetophenone was performed using 0.5 equivalents of catalyst precursor **C1a-c** in the presence of 3 equivalents of MeONa. Although the formation of Pd NPs was evidenced for the three complexes of **C1** family after catalytic tests (*vide supra*), Pd black formation was only observed when using **C1a** and **C1b** under these conditions. After separation of Pd black, the crude solutions were analyzed by MS-ESI (Figures S22-S24). In all cases, no peaks attributed to the reductive elimination of the ligand and the substrate were detected but double-charged species for **C1a** and **C1b** at *m/z* = 385.1533 and 399.1676, respectively (Figures S22-S23). We found that these peaks can be attributed to $[Pd(bisNHC)_2]^{2+}$ homoleptic tetracarbene species (Figures S25-S26). These cationic species were confirmed by independent synthesis according to Scheme 3 (Figures S36-S41) revealing an excellent agreement with observed fragmentation patterns in the MS-ESI spectra. Contrary to the assumption of strong M-NHC binding, these transformations are a clear demonstration of a controlled cleavage of the M-NHC bond, which could be a pivotal step for high-performance palladium catalysis.

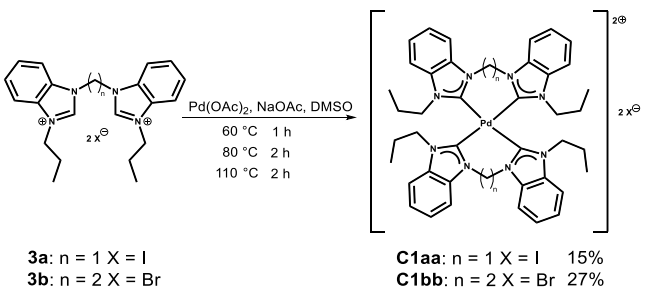


**Scheme 3.** Synthetic pathway for **C1aa** and **C1bb** complexes.

**Table 3. Conversion, TON and TOF values for the Suzuki-Miyaura reaction of *p*-haloacetophenone with phenylboronic acid in the presence of Hg.**

| Entry | Catalyst | *p*-iodoacetophenone | | | *p*-bromoacetophenone | | |
|---|---|---|---|---|---|---|---|
| | | 25 °C | | | 60 °C | | |
| | | Conv. | TON | TOF ($h^{-1}$) | Conv. | TON | TOF ($h^{-1}$) |
| 1 | **C1a** | 4 | 38 | 38 | 58 | 580 | 580 |
| 2 | **C1b** | 29 | 289 | 289 | 14 | 137 | 137 |
| 3 | **C1c** | 22 | 218 | 218 | 6 | 58 | 58 |
| 4 | **C2a** | 1 | 10 | 10 | 1 | 8 | 8 |
| 5 | **C2b** | 6 | 60 | 60 | 7 | 69 | 69 |
| 6 | **C2c** | 19 | 193 | 193 | 2 | 25 | 25 |
| 7 | **C3a** | 1 | 10 | 10 | 5 | 49 | 49 |
| 8 | **C3b** | 1 | 9 | 9 | 1 | 13 | 13 |
| 9 | **C3c** | 1 | 14 | 14 | 1 | 16 | 16 |
| 10 | **H-B** | 3 | 33 | 33 | 1 | 10 | 10 |

Reaction conditions: 8 x $10^{-4}$ mmol Pd, 0.8 mmol *p*-haloacetophenone, 1 mmol phenylboronic acid, 1.2 mmol MeONa, 2 mmol Hg, and 9 x $10^{-2}$ mmol naphthalene as an internal standard in 16 mL absolute EtOH. Conversion after 1 h reaction.

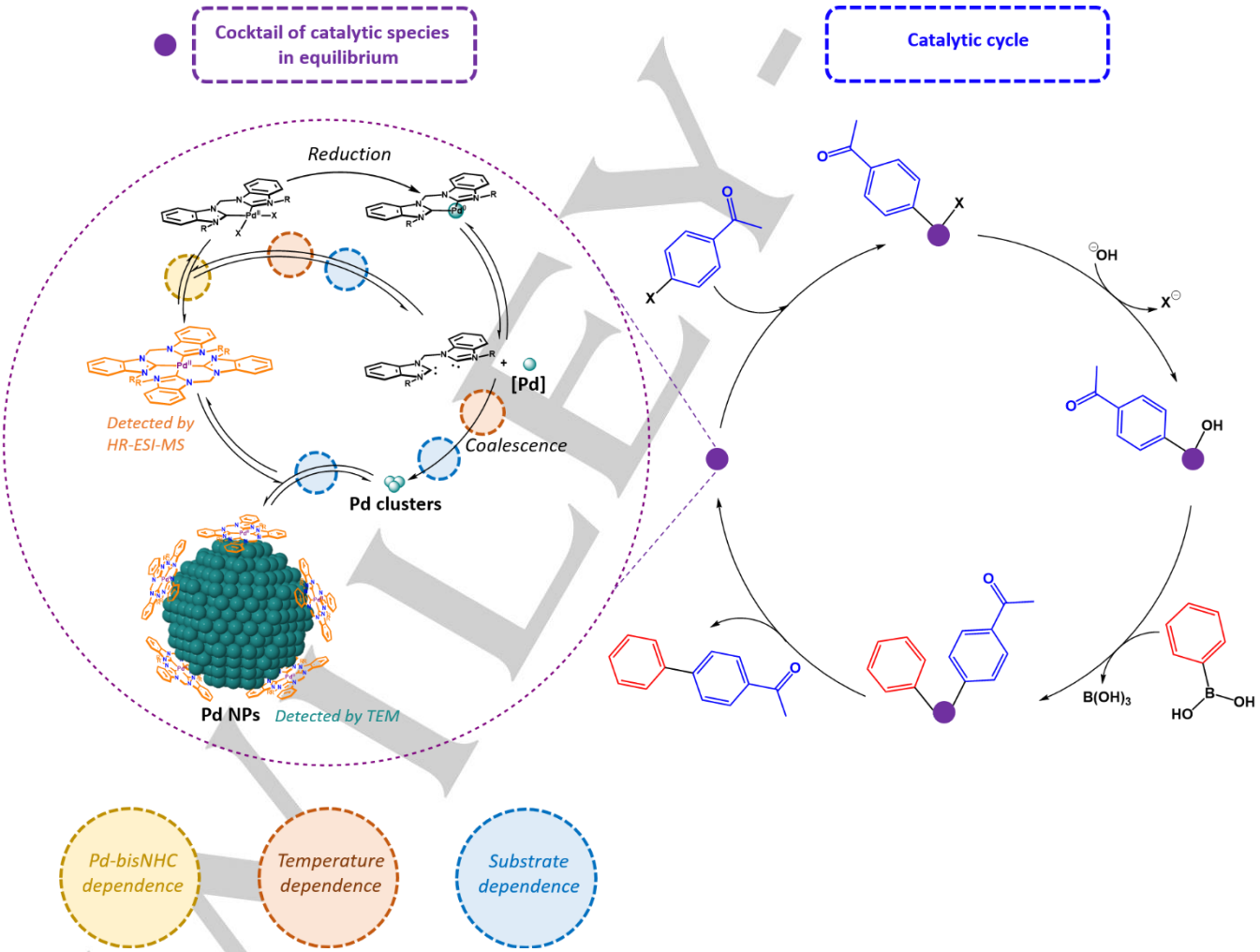


**Scheme 4.** Catalyst evolution and cationic Pd species-stabilized "Cocktail"-type mode of Suzuki-Miyaura reaction with Pd-bisNHC catalyst precursor.

On the basis of the obtained results and the good fit of their simulated ESI-MS spectra, we postulated that the reduction of these complexes followed by the oxidative addition of the aryl halide resulted in the formation of ionic species as proposed by Górna *et al*.[43] Such species can act as stabilizers of their first evolved Pd NPs (oxidative addition step) as well as a reservoir source enhancing catalyst turnover.

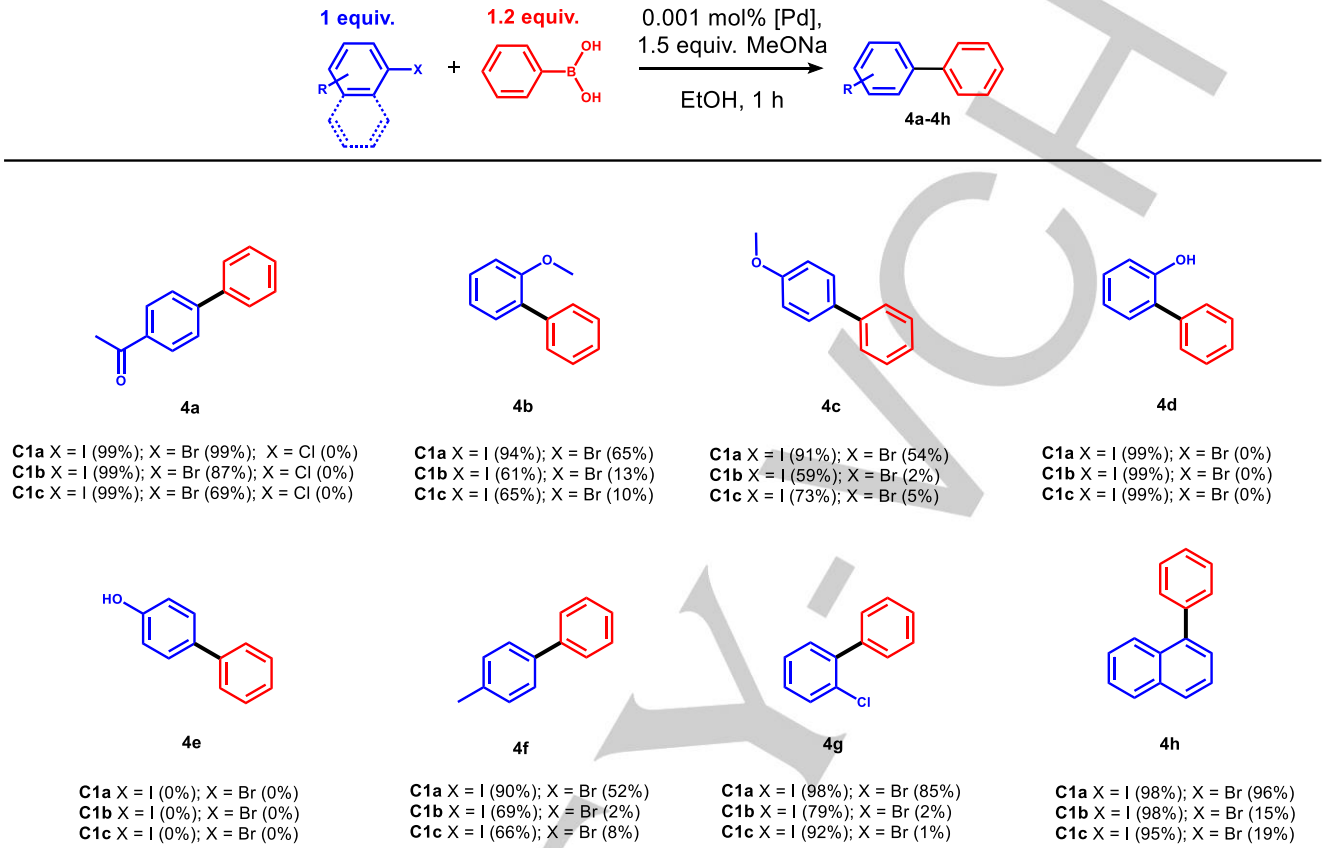


**Figure 7.** Reaction scope with the halogen X = I, Br or Cl in Ar-X and corresponding yields indicated under each product. The yields were determined by GC.

In fact, very recently, Eremin *et al.*[44] evidenced the formation of anionic palladium species in the Mizoroki-Heck reaction. However, no evidence for the formation of these anionic and dimeric palladium species was observed in our case (Figures S27-S29). Interestingly, the same results were observed when using *p*-bromoacetophenone (Figures S30-S35). Thus, the presence of the **C1aa** and **C1bb** double-charged cationic species generated from their respective **C1a** and **C1b** complexes could be explained through their enhanced formation by the pseudo-agostic and agostic interactions between the bridge –$CH_2$– protons and the palladium(II) core as already evidenced by the X-ray diffraction analyses of their **C1a** and **C1b** previous complexes (*vide supra*). From here, based on previous literature reports,[45] we propose a mechanism for the catalytic cycle (Scheme 4, right) in which a cocktail of catalytic species in equilibrium (Scheme 4, left) are evolved in the C-C coupling reaction. From here, "bisNHC-free" metal species are released from the [$PdX_2$(bisNHC)] precursors. Since these Pd species start to coalesce, the deattached bisNHC can react with the precursor under catalytic conditions (basic pH) to yield $[Pd(bisNHC)_2]^{2+}$ species. Thus, it could be expected that the homoleptic tetracarbene species govern the stabilization of evolving Pd NPs.

It is important to note that the catalytic performance of these systems strongly depends on the stability of Pd NPs against further aggregation to inactive Pd black. Then, the catalytic depletion experienced by **C1b** and **C1c** complexes when using *p*-bromoacetophenone (*vide supra*) could be attributed to the degradation of **C1bb** mediated by the catalytic conditions for the former and the absence of $[Pd(bisNHC)_2]^{2+}$ species for the latter. Thus, to further explore the role of these tetracarbene entities, both **C1aa** and **C1bb** complexes were tested as catalysts under the same conditions previously discussed (Figure S46 and Tables S4-S5). After observing that they catalyze the coupling of *p*-iodoacetophenone with phenylboronic acid at 60 °C (Figure S46a), it can be inferred that these species are in equilibrium in the cocktail of catalytic species (Scheme 4, left). However, decreasing the temperature to 25 °C (Figure S46b) reveals almost no conversion, indicating that once the **C1aa** and **C1bb** species are formed, they require an activation energy to participate in the catalytic reaction. Thus, these species act purely as stabilizing agent of the evolved Pd NPs at low temperatures. When **C1aa** and **C1bb** were used to catalyze the coupling of *p*-bromoacetophenone with phenyl boronic acid at 60 °C (Figure S46c), it can be observed that they start to catalyze after 20 min and 50 min, respectively. Then, these experiences prompt us to confirm that the formation of the tetracarbene homoleptic species is a dynamic process rather than static one under turnover conditions and that it is affected by the nature of the substrate used in the reaction.

**Scope of substrates.** To further explore the catalytic performance of the **C1a-c** complexes here prepared, a reaction scope for the Suzuki-Miyaura reaction was evaluated (Figure 7). Introducing electron-donating groups into the aryl iodides resulted in high product yields (**4b**, **4c**, **4f**, **4g**) for all **C1a-c** catalysts.

However, no product formation was observed for *para*-substituted iodophenols (**4e**). Additionally, the three catalysts demonstrated their applicability in the conversion of a steric substrate as for the case of 1-halogenonaphthalene (**4h**). From this scope of reactions, the **C1a** complex resulted the most active towards the C-C formation for both aryl iodides and bromides. Unfortunately, the activated *p*-chloroacetophenone substrate could not be activated resulting in an unsuccessful coupling.

## Conclusion

In conclusion, we have prepared and characterized a new series of NHC-based Pd(II) complexes as catalysts for the Suzuki-Miyaura reaction. Generally, in the presence of these catalysts, all reactions are carried out with good to excellent yields, and some quantitative yields can be achieve for aryl *p*-bromoacetophenone and *p*-iodoacetophenone. Moreover, most of the TOF values obtained for both *p*-iodoacetophenone and *p*-bromoacetophenone reactivity reached up to 12000 $h^{-1}$ at 0.1% catalyst loading under environmentally friendly and mild conditions.

We have demonstrated for the first time, a structure-activity relationship for palladium(II) complexes bearing bisNHC, bispyridyl and bisphosphine ligands in the Suzuki-Miyaura reaction. Firstly, Pd-release in the bulk media can be controlled by the nature of the selected bidentate ligands: an easier decoordination for bisphosphine ligands towards Pd NPs formation was observed compared to palladium(II) complexes bearing bispyridyl and even bisNHC ligands under same reaction conditions. Secondly, in general, longer bridges enhance overall catalyst performance but for bisNHC-based catalysts, shorter bridges are the responsible for catalyst perfomance enhancement. The catalytic studies, TEM analyses and mercury poisoning tests revealed that these enhanced catalytic activities could be ascribed to the formation of Pd NPs. Interestingly for **C1a** and **C1b** complexes, we evidenced that they initially evolved to $[Pd(bisNHC)_2]^{2+}$ species, which are proposed to be pivotal species involved in the catalytic cycle as NPs stabilizers and/or reservoir sources enhancing activities. A possible mechanism of the chemical transformation of the $[PdX_2(bisNHC)]$ complexes and formation of their corresponding homoleptic tetracarbene species is therefore presented here. Thirdly, it was also found that increasing the temperature could greatly enhance this initial catalytic activities due to a faster complex decomposition and further clusterification. Finally, the nature of the substrate has a strong influence in the catalytic activity since not only the C-Br bond is more difficult to activate, as expected, but also it controls the size and shape of evolved Pd NPs upon clusterification, playing as well a role in stabilization of formed Pd NPs.

These results will provide a new guideline for the design and applications of new catalysts. Upcoming work based on controlling the generation of expected highly-active catalytic moieties from **C1a-c** catalyst clusterification is under progress. More studies on the subject are anticipated in the near future to evaluate the stabilization of Pd NPs by tetracarbene homoleptic complexes.

## Experimental Section

**Materials and Methods.** GC analyses were performed on a Shimadzu Nexis GC-2030 gas chromatograph equipped with a FID detector, a HP-5 column (cross-linked 5% phenylmethylsiloxane, 30 m × 0.25 mm i.d. × 0.25 µm film thickness) with hydrogen as carrier gas. Yields were determined by GC based on the relative area of GC-signals referred to an internal standard (naphthalene) calibrated to the corresponding pure compounds.

Infrared (IR) spectra were recorded with a Thermo Scientific Nicolet iS5 spectrometer in the range 4000-525 cm-1 in attenuated total reflectance (ATR) mode.

$^{1}H$ NMR, $^{13}C$ NMR, $^{31}P\{1H\}$ NMR, HSQC and HMBC spectra were recorded on an Bruker Avance III 400 spectrometer at a temperature of 25 °C. All chemical shift values are given in ppm.

The palladium content was determined using a ICP-OES ACTIVA Jobin Yvon spectrometer from a solution obtained by treatment of the catalysts with sulfuric acid and aqua regia in a Teflon reactor at 400-450 °C.

Electrospray ionization Mass Spectrometry (ESI-MS) experiments were performed on a Bruker QTOF Impact II – instrument equipped with an UHPLC U3000 – Dionex by the Centre Commun de Spectrométrie de Masse from the University of Lyon.

Transmission electron microscopy (TEM) analyses were carried out on a JEOL 2010 microscope with an instrumental magnification of 50000x to 100000x and an acceleration voltage of 200kV. The point-to-point resolution of the microscope was 0.19 nm and the resolution between the lines was 0.14 nm. The microscope is equipped with an EDX link ISIS analyzer from Oxford instruments. Energy dispersive X-ray microanalysis (EDX) was conducted using a probe size 25-100 nm to analyze grains of the phases. The size distributions were determined via manual analysis of enlarged micrographs by measuring ca. 200 particles on a given grid to obtain a statistical size distribution and a mean diameter.

Crystals for the solid-state structures of the palladium **C1a-c** complexes could be obtained by slow evaporation of saturated solutions of the complexes in DMF or DMSO. Suitable single crystals were mounted on a nylon loop in perfluoroether oil on an Xcalibur, Atlas, Geminis ultra diffractometer. The crystals were keep at a steady T = 150.01(10) K during data collection. Data were measured using ω scans using $MoK_\alpha$ radiation. The total number of runs and images was based on the strategy calculation from the program CrysAlisPro.[46] The structures were solved with the SheIXT[47] structure solution program using Intrinsic Phasing solution method and by using Olex2[48] as a graphical interface. The models were refined with version 2018/3 of SheIXL using Least Squares minimization. All non-hydrogen atoms were refined anisotropically. Hydrogen atom positions were calculated geometrically and refined using the riding model.

**Catalytic Performance Studies for the Suzuki-Miyaura Reaction.** In glass tubes of a Radleys Carousel 12 Plus Station™ fitted with a water-cooled aluminum reflux head and septa, 16 mL of an absolute ethanol solution containing *p*-halogenoacetophenone (0.05 M), phenylboronic acid (0.06 M) and MeONa (0.075 M) were added. The reaction mixtures were stirred and heated at 60 °C or 25 °C under nitrogen atmosphere for 30 minutes. Thus, the palladium catalyst (8 x $10^{-4}$ mmol Pd) was added from a stock solution of the former (100 µL, 0.008 M in DMSO). The mixture was vigorously stirred and kept at 60 °C for 1 h under nitrogen. Then, an aliquot (*ca.* 0.5 mL) of the reaction crude was taken at different reaction times and quenched in a vial filled with water/ethyl acetate mixture (2:1.5, 3.5 mL) and with naphthalene (0.09 mmol) as standard. The organic phase was analyzed by GC and GC-MS. All products gave satisfactory data compared to reported literature {*p*-acetylbiphenyl [92-91-1], 2-methoxybiphenyl [86-26-0], 4-methoxybiphenyl [613-37-6], 4-phenyltoluene [644-08-6], 2-chloro-1,1-biphenyl [2051-60-7], 1-

phenylnaphthalene [605-02-7]}. For TEM analyses, a drop of the crude mixture was deposited under the holey carbon-covered copper. In order to obtain the iTOF values, the evolved mmol of *p*-acetylbiphenyl vs the time (in minutes) was plotted. Thus, a polynomial equation was fitted for the region 0-3 min and the first derivative was calculated. Finally, the iTOF values were obtained for x = 0 for the first derivative equation. TON values were calculated dividing the evolved mmol of p-acetylbiphenyl by 8 x $10^{-4}$ mmol of Pd. TOF values were calculated dividing the TON values by the required time (in hours) to achieve the maximum conversion for each catalyst.

**Synthesis and Characterization of the Ligands**

**1-propylbenzimidazole (*2*)**. A mixture of benzimidazole (8.86 g, 75 mmol, 1 eq), bromopropane (6.83 mL, 75 mmol, 1 eq) and potassium carbonate (20.73 g, 150 mmol, 2 eq) were refluxed in acetone (40 mL) overnight. After cooling to room temperature, the reaction mixture was filtered. The product was obtained as a yellow oil after removing the organic phase under reduced pressure. Yield: 10.42 g. 87%. The spectroscopic data are in accordance with that reported in the literature.[49]

**1,1'-Dipropyl-3,3'-methylenebisbenzimidazolium diiodide (*3a*).** In a sealed tube, a mixture of 1-propylbenzimidazole (1000 mg, 6.2 mmol, 2.1 eq) and diiodomethane (240 µL, 3.0 mmol, 1 eq) was heated at 120 °C for 4 h. After cooling to room temperature, acetonitrile (5 mL) was added to crush the solid by sonication. The crude precipitate was filtered off and washed with acetonitrile (5 mL x 2). The product was obtained as a pale white powder. Yield: 900 mg, 52%. $^1$H NMR (DMSO-$d_6$, 400 MHz, 25 °C) δ 0.97 (t, *J* = 7.03 Hz, 6H, $H_4$), 1.97 (m, 4H, $H_3$), 4.55 (t, *J* = 7.00 Hz, 4H, $H_2$), 7.40 (s, 2H, $H_{11}$), 7.79 (m, 4H, $H_7$ and $H_8$), 8.19 (d, *J* = 7.94 Hz, 2H, $H_9$), 8.39 (d, *J* = 8.23 Hz, 2H, $H_6$), 10.31 (s, 2H, $H_1$). $^{13}$C{$^1$H} NMR (DMSO-$d_6$, 100 MHz, 25 °C) δ 11.1 ($C_4$), 22.4 ($C_3$), 49.1 ($C_2$), 55.6 ($C_{11}$), 114.1 ($C_6$), 114.7 ($C_9$), 127.6 ($C_7$), 127.9 ($C_8$), 131.0 ($C_{10}$), 131.6 ($C_5$), 144.2 ($C_1$). (ATR) cm$^{-1}$: 1559 (ν(C=C), ν(C=N))ar, 1431 (δ(C=C), δ(C=N))ar, 1014 δ(C-H)ip, 751 δ(C-H)oop. HR-ESI-MS (DMSO): calculated: *m/z* = 461.1197 ([M-I]$^+$), found: *m/z* = 461.1188 ([M-I]$^+$).

**1,1'-Dipropyl-3,3'-(1,2-dimethylene)bisbenzimidazolium dibromide (*3b*).** In a sealed tube, a mixture of 1-propylbenzimidazole (641 mg, 4 mmol, 2 eq) and 1,2-dibromoethane (172 µL, 2.0 mmol, 1 eq) was heated at 120 °C for 4 h. After cooling to room temperature, acetonitrile (5 mL) was added to crush the solid by sonication. The crude precipitate was filtered off and washed with acetonitrile (5 mL x 2). The product was obtained as a pale white powder. Yield: 806 mg, 79%. $^1$H NMR ($D_2O$, 400 MHz, 25 °C) δ 0.82 (t, *J* = 7.29 Hz, 6H, $H_4$), 1.85 (m, 4H, $H_3$), 4.41 (t, *J* = 7.25 Hz, 4H, $H_2$), 5.24 (s, 4H, $H_{11}$), 7.38 (d, *J* = 8.67 Hz, 2H, $H_5$), 7.55 (t, *J* = 8.14 Hz, 2H, $H_7$), 7.68 (t, *J* = 7.91 Hz, 2H, $H_6$), 7.90 (d, *J* = 8.33 Hz, 2H, $H_8$), 9.41 (s, 2H, $H_1$). $^{13}$C{$^1$H} NMR ($D_2O$, 100 MHz, 25 °C) δ 10.1 ($C_4$), 22.0 ($C_3$), 46.4 ($C_{11}$), 49.0 ($C_2$), 111.6 ($C_5$), 113.9 ($C_8$), 127.6 ($C_6$), 127.7 ($C_7$), 131.0 ($C_9$), 131.2 ($C_{10}$), 141.1 ($C_1$). (ATR) cm$^{-1}$: 3012 ν(C-H)ar, 2938 ν(C-H), 1565 (ν(C=C), ν(C=N))ar, 1431 (δ(C=C), δ(C=N))ar, 1014 δ(C-H)ip, 751 δ(C-H)oop. HR-ESI-MS (DMSO): calculated: *m/z* = 427.1492 ([M-Br]$^+$); found: *m/z* = 427.1481 ([M-Br]$^+$), 174.1145 ([M-2Br]$^{+2}$).

**1,1'-Dipropyl-3,3'-(1,3-trimethylene)bisbenzimidazolium diiodide (*3c*).** In a sealed tube, a mixture of 1-propylbenzimidazole (801 mg, 5 mmol, 2 eq) and 1,3-diiodopropane (287 µL, 2.5 mmol, 1 eq) was heated at 130 °C for 30 min. After cooling to room temperature, acetonitrile (5 mL) was added to crush the solid by sonication. The crude white precipitate was filtered off and washed with acetonitrile (5 mL x 2). The product was obtained as a crude white powder. Yield: 1062 mg, 69%. $^1$H NMR (DMSO-$d_6$, 400 MHz, 25 °C) δ 0.97 (t, *J* = 7.39 Hz, 6H, $H_{14}$), 1.94 (m, 4H, $H_{13}$), 2.65 (m, 2H, $H_{11}$), 4.47 (t, *J* = 7.10 Hz, 4H, $H_{12}$), 4.69 (t, *J* = 7.29 Hz, 4H, $H_{10}$), 7.73 (m, 4H, $H_1$ and $H_5$), 8.13 (m, 4H, $H_2$ and $H_5$), 9.81 (s, 2H, $H_8$). $^{13}$C{$^1$H} NMR (DMSO-$d_6$, 100 MHz, 25 °C) 11.1 ($C_{14}$), 22.8 ($C_{13}$), 28.4 ($C_{11}$), 44.4 ($C_{10}$), 48.7 ($C_{12}$), 114.1 ($C_5$), 114.3 ($C_2$), 127.1 ($C_6$), 127.2 ($C_1$), 131.5 ($C_4$), 131.6 ($C_3$), 142.7 ($C_8$). (ATR) cm$^{-1}$: 1565 (ν(C=C), ν(C=N))ar, 1431 (δ(C=C), δ(C=N))ar, 1014 δ(C-H)ip, 751 δ(C-H)oop. HR-ESI-MS (DMSO): calculated: *m/z* = 489.1510 ([M-I]$^+$); found: *m/z* = 489.1497 ([M-I]$^+$).

**Synthesis and Characterization of the Complexes**

**Diiodido-(1,1'-dipropyl-3,3'-methylenedibenzimidazolin-2,2'-diylidene)palladium(II) (*C1a*).** Palladium(II) acetate (79 mg, 0.35 mmol, 1 eq) and ligand **3a** (210 mg, 0.36 mmol, 1.01 eq) were dissolved in degassed DMSO (3 mL) in a round-bottom flask. The reddish mixture was stirred for 4 h at room temperature, 17 h at 40 °C and, finally, 2 h at 120 °C. After cooling to room temperature, a yellow suspension was obtained. Filtration of the reaction mixture yielded the product as a greenish powder. Yield: 150 mg, 61%. $^1$H NMR (DMSO-$d_6$, 400 MHz, 25 °C): δ 0.83 (t, *J* = 6.4 Hz, 6H, $H_4$), 1.89 (m, 4H, $H_3$), 4.43 (m, 2H, $H_2$), 4.97 (m, 2H, $H_2$), 6.78 (d, *J* = 14.2 Hz, 1H, $H_{11}$), 7.45 (m, 5H, $H_7$, $H_8$ and $H_{11}$), 7.81 (d, *J* = 7.9 Hz, 2H, $H_9$), 8.27 (d, *J* = 7.9 Hz, 2H, $H_6$); $^{13}$C{$^1$H} NMR (DMSO-$d_6$, 100 MHz, 25 °C): δ 11.36 ($C_4$), 22.92 ($C_3$), 50.68 ($C_2$), 58.20 ($C_{11}$), 111.74 ($C_6$), 112.61 ($C_9$), 124.60 ($C_7$), 124.82 ($C_8$), 133.23 ($C_5$) 133.88 ($C_{10}$). IR (ATR) cm$^{-1}$: 3033 ν(C-H)ar, 2966 ν(C-H), 1414, 1388 (δ(C=C), δ(C=N))ar, 1040, 1014 δ(C-H)ip, 751 δ(C-H)oop. HR-ESI-MS (DMSO): calculated: *m/z* = 714.9026 ([M+Na]$^+$); found: *m/z* = 714.9020 ([M+Na]$^+$), 565.0075 ([M-I]$^+$). Note: C1, C2 and C11 are not observed in 1D spectrum. C11 and C2 are observed in HSQC.

**Dibromido-(1,1'-dipropyl-3,3'-ethylenedibenzimidazolin-2,2'-diylidene)palladium(II) (*C1b*).** Palladium(II) acetate (109 mg, 0.48 mmol, 1 eq) and ligand **3b** (250 mg, 0.49 mmol, 1.01 eq) were dissolved in degassed DMSO (3 mL) in a round-bottom flask. The reddish mixture was stirred for 4 h at room temperature, 17 h at 40 °C and, finally, 2 h at 120 °C. After cooling to room temperature, a greenish suspension was obtained. Filtration of the reaction mixture yielded the product as a pale yellow powder. Yield: 275 mg, 92%. $^1$H NMR (DMSO-$d_6$, 400 MHz, 25 °C): δ 0.98 (t, *J* = 7.2 Hz, 6H, $H_4$), 1.88 (m, 2H, $H_3$), 2.06 (m, 2H, $H_3$), 4.51 (m, 2H, $H_2$), 4.83 (m, 2H, $H_2$), 5.10 (m, 2H, $H_{10}$), 5.65 (m, 2H, $H_{10}$), 7.38 (m, 4H, $H_7$ and $H_7$), 7.75 (m, 4H, $H_5$ and $H_8$); $^{13}$C{$^1$H} NMR (DMSO-$d_6$, 100 MHz, 25 °C): δ 11.50 ($C_4$), 22.94 ($C_3$), 44.37 ($C_{10}$), 50.64 ($C_2$), 111.68 ($C_5$), 111.99 ($C_8$), 124.01 ($C_6$), 124.24 ($C_7$), 133.95 ($C_{11}$), 134.24 ($C_9$). (ATR) cm$^{-1}$: 3032 ν(C-H)ar, 2952 ν(C-H), 1443, 1390 (δ(C=C), δ(C=N))ar, 1053, 1013 δ(C-H)ip, 748 δ(C-H)oop. HR-ESI-MS (DMSO): calculated: *m/z* = 634.9442 ([M+Na]$^+$); found: *m/z* = 634.9433 ([M+Na]$^+$), 533.0358 ([M-Br]$^+$). Note: C1 is not observed

**Diiodido-(1,1'-dipropyl-3,3'-propylenedibenzimidazolin-2,2'-diylidene)palladium(II) (*C1c*).** Palladium(II) acetate (180 mg, 0.80 mmol, 1 eq) and ligand **3c** (500 mg, 0.81 mmol, 1.01 eq) were dissolved in degassed DMSO (3 mL) in a round-bottom flask. The reddish mixture was stirred for 4 h at room temperature, 17 h at 40 °C and, finally, 2 h at 120 °C. After cooling to room temperature, a yellowish suspension was obtained. Filtration of the reaction mixture yielded the product as a pale yellow powder. Yield: 345 mg, 60%. $^1$H NMR (DMSO-$d_6$, 400 MHz, 25 °C): δ 1.09 (t, *J* = 7.5 Hz, 6H, $H_9$), 1.80 (m, 2H, $H_8$), 1.99 (m, 1H, $H_{11}$), 2.15 (m, 2H, $H_8$), 2.62 (m, 1H, $H_{11}$), 4.51 (td, *J* = 4.79 Hz, *J* = 12.76 Hz, 2H, $H_7$), 4.74 (td, *J* = 5.19 Hz, *J* = 12.89 Hz, 2H, $H_7$), 4.88 (dd, *J* = 5.09 Hz, *J* = 14.90 Hz, 2H, $H_{10}$), 5.23 (dd, *J* = 11.94 Hz, *J* = 14.50 Hz, 2H, $H_{10}$), 7.30 (m, 4H, $H_2$ and $H_5$), 7.69 (m, 4H, $H_1$ and $H_6$); $^{13}$C{$^1$H} NMR (DMSO-$d_6$, 100 MHz, 25 °C): δ 11.11 ($C_9$), 21.37 ($C_8$), 29.30 ($C_{11}$), 48.82 ($C_{10}$), 50.24 ($C_7$), 110.7 ($C_1$), 111.7 ($C_6$), 123.20 ($C_2$), 123.40 ($C_5$), 133.12 ($C_3$), 134.04 ($C_4$). (ATR) cm$^{-1}$: 3033 ν(C-H)ar, 2938 ν(C-H), 1455, 1402 (δ(C=C), δ(C=N))ar, 1044, 1027 δ(C-H)ip, 742 δ(C-H)oop. HR-ESI-MS (DMSO): calculated: *m/z* = 742.9339 ([M+Na]$^+$); found: *m/z* = 742.9328 ([M+Na]$^+$), 593.0384 ([M-I]$^+$). Note: C12 is not observed

**Bis(1,1'-dipropyl-3,3'-methylenedibenzimidazolin-2,2'-diylidene)palladium(II) iodide (*C1aa*).** Palladium(II) acetate (29 mg, 0.13 mmol, 1 eq), ligand **3a** (163 mg, 0.28 mmol, 2.1 eq) and sodium acetate

(21.6 mg, 0.26 mmol, 2 eq) were dissolved in degassed DMSO (3 mL) in a round-bottom flask. The brownish mixture was stirred for 1 h at 60 °C, 2 h at 80 °C and 1 h at 110 °C. Thus, sodium acetate (21.6 mg, 0.26 mmol, 2 eq) was added again and the reaction mixture was kept at 110 °C for 1.5 h. After cooling to room temperature, a yellowish suspension was obtained. Water (6 mL) was added to precipitate a pale yellow powder. The precipitate was filtered and washed with acetone (6 mL x 6). The product was obtained as a white powder. Yield: 20 mg, 15%. $^1$H NMR (DMSO-$d_6$, 400 MHz, 25 °C): δ 0.54 (t, $J$ = 7.21 Hz, 12H, $H_4$), 1.54 (m, 4H, $H_3$), 1.76 (m, 4H, $H_3$), 3.60 (m, 4H, $H_2$), 4.33 (m, 4H, $H_2$), 7.00 (d, $J$ = 14.49 Hz, 2H, $H_{11}$), 7.51 (t, $J$ = 7.82 Hz, 4H, $H_7$), 7.62 (t, $J$ = 8.09 Hz, 4H, $H_8$), 7.64 (d, $J$ = 14.03 Hz, 2H, $H_{11}$), 7.86 (d, $J$ = 8.22 Hz, 4H, $H_9$), 8.52 (d, $J$ = 8.28 Hz, 4H, $H_6$); $^{13}$C{$^1$H} NMR (DMSO-$d_6$, 100 MHz, 25 °C): δ 10.95 ($C_4$), 22.75 ($C_3$), 49.72 ($C_2$), 57.92 ($C_{11}$), 111.83 ($C_6$), 112.62 ($C_9$), 124.53 ($C_7$), 124.86 ($C_8$), 133.35 ($C_5$), 133.62 ($C_{10}$), 178.87 ($C_1$). (ATR) cm$^{-1}$: 3025 ν(C-H)ar, 2965 ν(C-H), 1450, 1395 (δ(C=C), δ(C=N))ar, 1051, 1017 δ(C-H)ip, 755 δ(C-H)oop. HR-ESI-MS (DMSO): calculated: $m/z$ = 385.1520 ([M-2I$^-$]$^{2+}$); found: $m/z$ = 385.1514 ([M-2I$^-$]$^{2+}$), 897.2086 ([M-I$^-$]$^+$).

**Bis(1,1'-dipropyl-3,3'-ethylenedibenzimidazolin-2,2'-diylidene)palladium(II) bromide (*C1bb*).** Palladium(II) acetate (33 mg, 0.15 mmol, 1 eq), ligand **3b** (157 mg, 0.30 mmol, 2.1 eq) and sodium acetate (24 mg, 0.29 mmol, 2 eq) were dissolved in degassed DMSO (3 mL) in a round-bottom flask. The brownish mixture was stirred for 1 h at 60 °C, 2 h at 80 °C and 1 h at 110 °C. Thus, sodium acetate (24 mg, 0.3 mmol, 2 eq) was added again and the reaction mixture was kept at 110°C for 1.5 h. After cooling to room temperature, a white suspension was obtained. Water (6 mL) was added to precipitate a grey powder. The precipitate was filtered and washed with acetone (6 mL x 6). The product was obtained as a pale grey powder. Yield: 38 mg, 27%. $^1$H NMR ($CD_3OD$, 400 MHz, 25 °C): δ 0.75 (t, $J$ = 7.22 Hz, 12H, $H_4$), 0.87 (m, 4H, $H_3$), 1.75 (m, 4H, $H_3$), 4.23 (m, 4H, $H_2$), 4.42 (m, 4H, $H_2$), 5.50 (m, 4H, $H_{11}$), 5.83 (m, 4H, $H_{11}$), 7.45 (td, $J$ = 0.87 Hz, $J$ = 7.35 Hz, 4H, $H_7$), 7.52 (dt, $J$ = 0.98 Hz, $J$ = 7.52 Hz, 4H, $H_8$), 7.64 (d, $J$ = 7.96 Hz, 4H, $H_9$), 7.90 (d, $J$ = 8.21 Hz, 4H, $H_6$); $^{13}$C{$^1$H} NMR ($CD_3OD$, 100 MHz, 25 °C): δ 11.36 ($C_4$), 23.97 ($C_3$), 46.29 ($C_{11}$), 51.95 ($C_2$), 112.31 ($C_6$), 113.10 ($C_9$), 126.20 ($C_8$), 126.24 ($C_7$), 135.13 ($C_5$), 135.82 ($C_{10}$), 176.26 ($C_1$). (ATR) cm$^{-1}$: 3026 ν(C-H)ar, 2965 ν(C-H), 1451, 1395 (δ(C=C), δ(C=N))ar, 1040, 1014 δ(C-H)ip, 765 δ(C-H)oop. HR-ESI-MS ($CH_3OH$): calculated: $m/z$ = 399.1677 ([M-2Br$^-$]$^{2+}$); found: $m/z$ = 399.1693 ([M-2Br$^-$]$^{2+}$).

## Appendix A

CCDC 2007730 (for **3b**), 2007729 (for **C1a**), 2007731 (for **C1b**) and 2007732 (for **C1c**); contains the supplementary crystallographic data for this paper. These data can be obtained free of charge from The Cambridge Crystallographic Data Centre via www.ccdc.cam.ac.uk/data_request/cif.

## Acknowledgements

Support from ANR (HYPERCAT, contract N° ANR-18-CE07-0021-03) research program ''HYPERCAT'' is gratefully acknowledged. We kindly acknowledge the 'Analytical Platform'' of IRCELYON, Centre Commun de Spectrométrie de Masse of University Lyon 1 for analyses and helpful discussions (L. Burel for TEM and N. Bonnet and P. Mascunan for ICP-OES analyses). We also thank E. Jeanneau for X-ray diffraction studies.

**Keywords:** Palladium • Catalysis • C-C coupling • Carbenes • Nanoparticles

[1] S. Kotha, K. Lahiri, D. Kashinath, *Tetrahedron* **2002**, *58*, 9633-9695.
[2] A. Ganesan, *Drug Discov. Today* **2001**, *6*, 238-241.
[3] a) D. Sanhes, E. Raluy, S. Retory, N. Saffon, E. Teuma, M. Gómez, *Dalton Trans.* **2010**, *39*, 9719-9726; b) F. Gómez-Villarraga, J. De Tovar, M. Guerrero, P. Nolis, T. Parella, P. Lecante, N. Romero, L. Escriche, R. Bofill, J. Ros, X. Sala, K. Philippot, J. García-Antón, *Dalton Trans.* **2017**, *46*, 11768-11778; c) I. Favier, D. Pla, M. Gómez, *Chem. Rev.* **2020**, *120*, 1146-1183.
[4] A. Fihri, M. Bouhrara, B. Nekoueishahraki, J.-M. Basset, V. Polshettiwar, *Chem. Soc. Rev.* **2011**, *40*, 5181-5203.
[5] A. F. Schmidt, A. A. Kurokhtina, *Kinet. Catal.* **2012**, *53*, 714-730.
[6] L. Djakovitch, K. Koehler, J. G. De Vries, in The Role of Palladium Nanoparticles as Catalyst for Carbon – Carbon Coupling Reactions. In *Nanoparticles and Catalysis* (Editor: D. Astruc), Wiley-VCH, Weinheim, **2008**, pp. 303-348.
[7] D. Cantillo, C. O. Kappe, *ChemCatChem* **2014**, *6*, 3286-3305.
[8] a) R. K. Arvela, N. E. Leadbeater, M. J. Collins, *Tetrahedron* **2005**, *61*, 9349-9355; b) J. Durand, E. Teuma, M. Gómez, *Eur. J. Inorg. Chem.* **2008**, 3577-3586; c) I. Favier, D. Madec, E. Teuma, M. Gómez, *Curr. Org. Chem.* **2011**, *15*, 3127-3174; d) V. M. Chernyshev, E. A. Denisova, D. B. Eremin. V. P. Ananikov, *Chem. Sci.* **2020**, doi.org/10.1039/D0SC02629H
[9] R. H. Morris, *Acc. Chem. Res.* **2015**, *48*, 1494-1502.
[10] P. W. N. M. Van Leeuween, P. C. J. Kamer, J. N. H. Reek, P. Dierkes, *Chem. Rev.* **2000**, *100*, 2741-2770.
[11] Y. Liang, Y. Li, H. Wang, J. Zhou, J. Wang, T. Regier, H. Dai, *Nat. Mater.* **2011**, *10*, 780-786.
[12] Y. B. Dudkina, K. V. Kohlin, T. V. Gryaznova, D. R. Islamov, O. N. Kataeva, I. Kh. Rizvanov, A. I. Levitskaya, O. D. Fominykh, M. Y. Balakina, O. G. Sinyashin, Y. H. Budnikova, *Dalton Trans.* **2017**, *46*, 165-177.
[13] R. Matheu, P. Garrido-Barros, M. Gil-Sepulcre, M. Z. Ertem, X. Sala, C. Gimbert-Suriñach, A. Llobet, *Nat. Chem. Rev.* **2019**, *3*, 331-341.
[14] G. D. Frey, V. Lavallo, B. Donnadieu, W. W. Schoeller, G. Bertrand, *Science* **2007**, *316*, 439-441.
[15] Y. Wang, Y. Xie, P. Wei, R. B. King, H. F. Schaefer III, P. V. R. Schleyer, G. Robinson, *Science* **2008**, *321*, 1069-1071.
[16] H. M. Lee, C. Y. Lu, C. Y. Chen, C. W. Chen, H. C. Lin, P. L. Chiu, P. L. P. Y. Cheng, *Tetrahedron* **2004**, *60*, 5807-5825.
[17] T. Scherg, S. K. Schneider, G. D. Frey, J. Schwarz, E. Herdtweck, W. A. Herrmann, *Synlett* **2006**, *18*, 2894-2907.
[18] M. V. Baker, B. W. Skelton, A. H. White, C. C. Williams, *J. Chem. Soc. Dalton Trans.* **2001**, *2*, 111-120.
[19] M. V. Baker, D. H. Brown, P. V. Simpson, B. W. Skelton, A. H. White, C. C. Williams, *J. Organomet. Chem.* **2006**, *691*, 5848-5855.
[20] M. V. Baker, D. H. Brown, P. V. Simpson, B. W. Skelton, A. H. White, *Dalton Trans*. **2009**, *35*, 7294-7307.
[21] R. Jothibasu, H. V. Huynh, *J. Organomet. Chem*. **2011**, *696*, 3369-3375.
[22] W. A. Herrmann, C.-P. Reisinger, M. Spielger, *J. Organomet. Chem.* **1998**, *557*, 93-96.
[23] C. Zhang, M. L. Trudell, *Tetrahedron Lett*. **2000**, *41*, 595-598.
[24] S. Ahrens, A. Zeller, M. Taige, T. Strassner, *Organometallics* **2006**, *25*, 5409-5415.
[25] W. L. Steffen, G. J. Palenik, *Inorg. Chem.* **1976**, *15*, 2432-2439.
[26] J. Berding, M. Lutz, A. L. Spek, E. Bouwman, *Organometallics* **2009**, *28*, 1845-1854.
[27] F. E. Hahn, T. von Fehren, T. Lügger, *Inorg. Chim. Acta* **2005**, *358*, 4137-4144.
[28] M. Brookhart, M. L. H. Green, G. Parkin, *PNAS* **2007**, *104*, 6908-6914.
[29] S. E. Livingstone, *J. Proc. R. Soc. N. S. Wales* **1952**, *86*, 32-37.
[30] G. R. Newkome, V. K. Gupta, H. C. R. Taylor, F. R. Fronczek, *Organometallics* **1984**, *3*, 1549-1554.
[31] M. Beller, H. Fischer, W. A. Herrmann, K. Öfele, C. Broβmer, *Angew. Chem. Int. Ed. Engl.* **1995**, *34*, 1848-1849.
[32] S. J. Blanksby, G. B. Ellison, *Acc. Chem. Res.* **2003**, *36*, 255-263.

[33] J. Louie, J. F. Hartwig, *Angew. Chem. Int. Ed. Engl.* **1996**, *35*, 2359-2361.
[34] A. V. Astakhov, O. V. Khazipov, A. Y. Chernenko, D. V. Pasyukov, A. S. Kashin, E. G. Gordeev, V. N. Khrustalev, V. M. Chernyshev, V. P. Ananikov, *Organometallics* **2017**, *36*, 1981-1992.
[35] a) S. C. Sau, S. Santra, T. T. Sen, S. K. Mandal, D. Koley, *Chem. Commun.* **2012**, *48*, 555-557; b) I. Favier, P. Lavedan, S. Massou, E. Teuma, K. Philippot, B. Chaudret, M. Gómez, *Top. Catal.* **2013**, *56*, 1253-1261 ; c) H. Xie, L. Zhao, L. Yang, Q. Lei, W. Fang, C. Xiong, *J. Org. Chem*, **2014**, *79*, 4517-4527; d) R. Jagadeesan, G. Velmurugan, P. Venuvanalingam, *RSC Adv.* **2015**, *5*, 80661-80667.
[36] J. M. Hayes, M. Viciano, E. Peris, G. Ujaque, A. Lledós, *Organometallics* **2007**, *26*, 6170-6183.
[37] D. Nemcsok, K. Wichmann, G. Frenking, *Organometallics* **2004**, *23*, 3640-3646.
[38] D. M. Khramov, V. M. Lynch, C. W. Bielawski, *Organometallics* **2007**, *26*, 6042-6049.
[39] C. A. Tolman, *Chem. Rev.* **1977**, *77*, 313-348.
[40] L. M. Rossi, J. L. Fioro, M. A. S. Garcia, C. P. Ferraz, *Dalton Trans.* **2018**, *47*, 5889-5915.
[41] G. M. Whitesides, M. Hackett, R. L. Brainard, J. P. P. M. Lavalleye, A. F. Sowinski, A. N. Izumi, S. S. Moore, D. W. Brown, E. M. Staud, *Organometallics* **1985**, *4*, 1819-1830.
[42] R. L. Oliveira, W. He, R. J. M. Klein Gebbink, K. P. de Jong, *Catal. Sci. Technol.* **2015**, *5*, 1919-1928.
[43] M. Górna, M. S. Szulmanowicz, A. Gniewek, W. Tylus, A. M. Trzeciak, *J. Organomet. Chem.* **2015**, *785*, 92-99.
[44] D. E. Eremin, E. A. Denisova, A. Y. Kostyukovich, J. Martens, G. Berden, J. Oomens, V. N. Khrustalev, V. M. Chernyshev, V. P. Ananikov, *Chem. Eur. J.* **2019**, *25*, 16564-16572.
[45] a) C. Amatore, G. Le Duc, A. Jutand, *Chem. Eur. J.* **2013**, *19*, 10082-10093; b) M. A. Ortuño, A. Lledós, F. Maseras, G. Ujaque *ChemCatChem* **2014**, *6*, 3132-3138; c) A. A. Thomas, A. F. Zahrt, C. P. Delaney, S. E. Denmark *J. Am. Chem. Soc.* **2018**, *140*, 4401-4416.
[46] CrysAlisPro Software System, version 1.171.40.53. Rigaku Oxford Diffraction, **2019**.
[47] G. M. Sheldrick, *Acta Cryst.* **2015**, *71*, 3-8.
[48] O. V. Dolomanov, L. J. Bourhis, R. J. Gildea, J. A. K. Howard, H. Puschmann, *J. Appl. Cryst.* **2009**, *42*, 339-341.
[49] Y.-R. Lin, C.-C. Chiu, H.-T. Chiu; D.-S. Lee, T.-J. Lu, *Appl. Organometal. Chem.* **2018**, *32*.

10.1002/cctc.202001253





## Entry for the Table of Contents

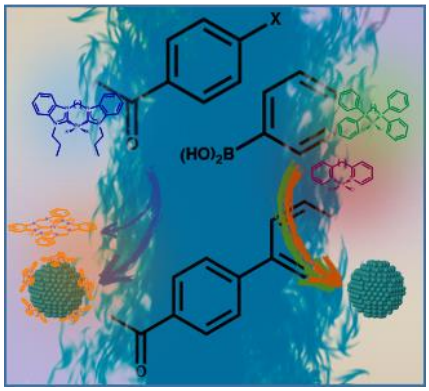


The structure-activity relationship for palladium(II) complexes bearing bisNHC, bispyridyl and bisphosphine ligands in the Suzuki-Miyaura reaction have been studied. Two bisNHC-based complexes form homoleptic tetracarbene species, which are proposed to be pivotal species involved in the catalytic cycle. In addition, a scheme of the mechanism of chemical transformation for these elucidated entities have been proposed.